

# Quest for magicity in hypernuclei

M. Ikram<sup>1</sup>, Bharat Kumar<sup>2</sup>, S. K. Biswal<sup>2</sup> and S. K. Patra<sup>2</sup>

<sup>1</sup> *Department of Physics, Aligarh Muslim University, Aligarh-202002, India*

<sup>2</sup> *Institute of Physics, Sachivalaya Marg, Bhubaneswar-751005, India.\**

(Dated: April 30, 2019)

In present study, we search the lambda magic number in hypernuclei within the framework of relativistic mean field theory (RMF) with inclusion of hyperon-nucleon and hyperon-hyperon potentials. Based on one- and two-lambda separation energy and two-lambda shell gap; 2, 8, 14, 18, 20, 28, 34, 40, 50, 58, 68, 70 and 82 are suggested to be the  $\Lambda$  magic number within the present approach. The weakening strength of  $\Lambda$  spin-orbit interaction is responsible for emerging the new lambda shell closure other than the model scheme. The predicted  $\Lambda$  magic numbers are in remarkable agreement with earlier predictions and hypernuclear magicity quite resembles with nuclear magicity. Our results are supported by nuclear magicity, where neutron number  $N = 34$  is experimentally observed as a magic which is one of the  $\Lambda$  closed shell in our predictions. In addition, the stability of hypernuclei is also examined by calculating the binding energy per particle, where Ni hypernucleus is found to be most tightly bound triply magic system in considered hypernuclei. Nucleon and lambda density distributions are observed and it is found that introduced  $\Lambda$ 's have significant impact on total density and reduces the central depression of the core nucleus. Nucleon and lambda mean field potentials and spin-orbit interaction potentials are also observed for predicted triply magic hypernuclei and the addition of  $\Lambda$ 's affect the both the potentials to a large extent. The single-particle energy levels are also analyzed to explain the shell gaps for triply magic multi- $\Lambda$  hypernuclei.

PACS numbers: 21.10.-k, 21.10.Dr, 21.80.+a

## I. INTRODUCTION

The study of hypernuclei has been attracting great interest of nuclear physics community in providing the information from nucleon-nucleon (NN) interaction to hyperon-nucleon (YN) and hyperon-hyperon (YY) interactions. Due to the injection of hyperons a new dimension is added in normal nuclear system and hyperons serve as a potential probe for exploring many nuclear properties in domain of strangeness [1–3]. However, hyperon-nucleon interaction is weaker than nucleon-nucleon but it is imperative as well as important to describe the nuclear many-body system with strangeness. Various theoretical approaches Skyrme Hartree Fock [4–12], relativistic mean field [13–18], cluster, variational, diffusion Monte Carlo [19–29], and G-matrix [30–32] have been employed by scientific community to estimate the strength of hyperon-nucleon as well hyperon-hyperon interactions. Further, these models have established themselves as very effective in testing the existence of bound hypernuclei and the stability of nucleonic core against hyperon(s) addition or the occurrence of exotic strange matter which facilitate the path toward multi-strange systems.

Magic numbers in nuclear physics are certain neutron and proton numbers in atomic nuclei, in which higher stability in the ground state is observed than in the neighbouring nuclides and are most abundant in nature. The various experimental signatures that show discontinuity at magic numbers are: the energy required for the separation of one and two nucleons, the energies of alpha and beta transitions, pairing energy and the excitation of low-lying vibrational [33–35]. The separa-

tion energy is sensitive to the collective or single particle interplay and provides a sufficient information about the nuclear structure effects. The discovery of magic numbers paved the way to great progress in understanding of nuclear structure and these numbers became the cornerstones for future theoretical developments in nuclear physics.

It is worthy to mention that the several signatures are seen for the evolution of the magic gaps along the nuclear chart including superheavy region [36–38]. The quest for proton or neutron magic numbers in the elusive mass region of superheavy nuclei is of utmost importance as the mere existence of superheavy nuclei is the result of the interplay between the attractive nuclear force (shell effects) and the large disruptive coulomb repulsion between the protons that favours the fission [39, 40]. It is well established that 2, 8, 20, 28, 50, 82 and 126 are the nucleonic magic number. In addition to this,  $Z = 120$  and  $N = 172, 184$  are predicted to be next magic number by various theoretical models in superheavy mass region [41–45]. These predictions have been made on the basis of separation energy, shell gaps, pairing energy and shell correction energy etc. It may therefore relevant to extend the line of thought to the hypernuclear chart. It is well known that the spin-orbit interaction in  $\Lambda$  channel is weaker than nucleonic sector and thus the  $\Lambda$  magic numbers are expected to be close to the harmonic oscillator ones: 2, 8, 20, 40 and 70. In this paper, our main motive is to make an extensive investigation to search the  $\Lambda$  magic number within the RMF approach and to obtain the stability of triply magic system with doubly magic core.

The magic numbers in nuclei are characterized by a large shell gap in single-particle energy levels. This means that the nucleon in the lower level has a comparatively large value of energy than that on higher level giving rise to more stability. The extra stability corresponding to certain number can be estimated from the sudden fall in the separation energy. The

\*Electronic address: [ikram@iopb.res.in](mailto:ikram@iopb.res.in)

$\Lambda$  separation energy is considered to be one of the key quantity to reveal the nuclear response to the addition of lambda hyperon. Therefore, in present work, we obtain the the binding energy per particle and one-lambda as well as two-lambda separation energies for considered multi-hypernuclei. Moreover, two-lambda shell gaps is also calculated to make the clear presentation of the magic number which also support to the two-lambda separation energy. To mark the  $\Lambda$  shell gaps, single-particle energy levels are analyzed that may correspond to  $\Lambda$  magic number. In addition, to analyze the structural distribution as well as impact of  $\Lambda$  hyperon on bubble structure for considered nuclei, total (nucleon plus  $\Lambda$ ) density is reported. Nucleon and lambda mean field and spin-orbit interaction potentials are also observed. On the basis of binding energy per particle, the stability of triply magic hypernuclei is reported.

RMF theory has been quite successful for studying the infinite nuclear systems and finite nuclei including the super-heavy mass region [41–52]. It is quite successful to study the equation of state for infinite nuclear matter as well as pure neutron matter, where the existence of strange baryons is expected [53, 54]. In this context, addition of strangeness degree of freedom to RMF formalism is obvious for the suitable expansion of the model and such type of attempts have already been made [54–65]. RMF explains not only the structural properties of singly strange hypernuclei but also provides the details study of multi-strange systems containing several  $\Lambda$ 's,  $\Sigma$ 's or  $\Xi$ 's. In fact, RMF explains spin-orbit interaction very nicely in normal nuclei as well as hypernuclei. The contribution of spin-orbit interaction is very crucial in emerging the magic number in nucleonic sector and the same is expected in strange sector.

The paper is organized as follows: A brief introduction on hypernuclei and magic number is given in Section I. Section II gives a brief description of relativistic mean field formalism for hypernuclei with inclusion of  $\Lambda N$  and  $\Lambda\Lambda$  interactions. The results are presented and discussed in Section III. The paper is summarized in Section IV.

## II. FORMALISM

Relativistic mean field theory has been applied successfully to study the structural properties of normal nuclei as well as hypernuclei [55–57, 59, 60, 63–65]. The suitable expansion to hypernuclei has been made by including the lambda-baryon interaction Lagrangian with effective  $\Lambda N$  potential. The total Lagrangian density for single- $\Lambda$  hypernuclei has been given in many Refs. [55–57, 59, 60, 63–65]. For dealing the multi-lambda hypernuclei in quantitative way, the additional strange scalar ( $\sigma^*$ ) and vector ( $\phi$ ) mesons have been included which simulate the  $\Lambda\Lambda$  interaction [54, 58, 61, 62]. Now, the total Lagrangian density can be written as

$$\mathcal{L} = \mathcal{L}_N + \mathcal{L}_\Lambda + \mathcal{L}_{\Lambda\Lambda}, \quad (1)$$

$$\begin{aligned} \mathcal{L}_N &= \bar{\psi}_i \{ i\gamma^\mu \partial_\mu - M \} \psi_i + \frac{1}{2} (\partial^\mu \sigma \partial_\mu \sigma - m_\sigma^2 \sigma^2) - \frac{1}{3} g_2 \sigma^3 \\ &\quad - \frac{1}{4} g_3 \sigma^4 - g_s \bar{\psi}_i \psi_i \sigma - \frac{1}{4} \Omega^{\mu\nu} \Omega_{\mu\nu} + \frac{1}{2} m_\omega^2 \omega^\mu \omega_\mu \\ &\quad - g_\omega \bar{\psi}_i \gamma^\mu \psi_i \omega_\mu - \frac{1}{4} B^{\mu\nu} B_{\mu\nu} + \frac{1}{2} m_\rho^2 \vec{\rho}^\mu \vec{\rho}_\mu - \frac{1}{4} F^{\mu\nu} F_{\mu\nu} \\ &\quad - g_\rho \bar{\psi}_i \gamma^\mu \vec{\tau} \psi_i \vec{\rho}^\mu - e \bar{\psi}_i \gamma^\mu \frac{(1 - \tau_{3i})}{2} \psi_i A_\mu, \\ \mathcal{L}_\Lambda &= \bar{\Psi}_\Lambda \{ i\gamma^\mu \partial_\mu - m_\Lambda \} \Psi_\Lambda - g_{\sigma\Lambda} \bar{\Psi}_\Lambda \Psi_\Lambda \sigma - g_{\omega\Lambda} \bar{\Psi}_\Lambda \gamma^\mu \Psi_\Lambda \omega_\mu, \\ \mathcal{L}_{\Lambda\Lambda} &= \frac{1}{2} (\partial^\mu \sigma^* \partial_\mu \sigma^* - m_{\sigma^*}^2 \sigma^{*2}) - \frac{1}{4} S^{\mu\nu} S_{\mu\nu} + \frac{1}{2} m_\phi^2 \phi^\mu \phi_\mu \\ &\quad - g_{\sigma^*\Lambda} \bar{\Psi}_\Lambda \Psi_\Lambda \sigma^* - g_{\phi\Lambda} \bar{\Psi}_\Lambda \gamma^\mu \Psi_\Lambda \phi_\mu, \end{aligned} \quad (2)$$

where  $\psi$  and  $\Psi_\Lambda$  denote the Dirac spinors for nucleon and  $\Lambda$ -hyperon, whose masses are  $M$  and  $m_\Lambda$ , respectively. Because of zero isospin, the  $\Lambda$ -hyperon does not couple to  $\rho$ -mesons. The quantities  $m_\sigma$ ,  $m_\omega$ ,  $m_\rho$ ,  $m_{\sigma^*}$ ,  $m_\phi$  are the masses of  $\sigma$ ,  $\omega$ ,  $\rho$ ,  $\sigma^*$ ,  $\phi$  mesons and  $g_s$ ,  $g_\omega$ ,  $g_\rho$ ,  $g_{\sigma\Lambda}$ ,  $g_{\omega\Lambda}$ ,  $g_{\sigma^*\Lambda}$ ,  $g_{\phi\Lambda}$  are their coupling constants, respectively. The nonlinear self-interaction coupling of  $\sigma$  mesons is denoted by  $g_2$  and  $g_3$ . The total energy of the system is given by  $E_{total} = E_{part}(N, \Lambda) + E_\sigma + E_\omega + E_\rho + E_{\sigma^*} + E_\phi + E_c + E_{pair} + E_{c.m.}$ , where  $E_{part}(N, \Lambda)$  is the sum of the single-particle energies of the nucleons (N) and hyperon ( $\Lambda$ ). The energies parts  $E_\sigma$ ,  $E_\omega$ ,  $E_\rho$ ,  $E_{\sigma^*}$ ,  $E_\phi$ ,  $E_c$ ,  $E_{pair}$  and  $E_{c.m.}$  are the contributions of meson fields, Coulomb field, pairing energy and the center-of-mass energy, respectively. In present work, for meson-baryon coupling constant, NL3\* parameter set is used through out the calculations [66]. To find the numerical values of used  $\Lambda$ -meson coupling constants, we adopt the nucleon coupling to hyperon couplings ratio defined as;  $R_\sigma = g_{\sigma\Lambda}/g_s$ ,  $R_\omega = g_{\omega\Lambda}/g_\omega$ ,  $R_{\sigma^*} = g_{\sigma^*\Lambda}/g_s$  and  $R_\phi = g_{\phi\Lambda}/g_\omega$ . The relative coupling values are used as  $R_\omega = 2/3$ ,  $R_\phi = -\sqrt{2}/3$ ,  $R_\sigma = 0.621$  and  $R_{\sigma^*} = 0.69$  [61, 67, 68]. In present calculations, we use the constant gap BCS approximation to include the pairing interaction and the centre of mass correction is included by  $E_{c.m.} = -(3/4)41A^{-1/3}$ .

## III. RESULTS AND DISCUSSIONS

Before taking a detour on searching the  $\Lambda$  magic behaviour in multi- $\Lambda$  hypernuclei, first we see the effects of introduced  $\Lambda$  hyperon on normal nuclear core; how the binding energy and radii of normal nuclear system is affected by addition of  $\Lambda$ 's? To analyze this, we consider a list of normal nuclei covering a range from light to superheavy mass region i.e.  $^{16}\text{O}$  to  $^{378}\text{120}$ . Total binding energy (BE), binding energy per particle (BE/A), lambda binding energy ( $B_\Lambda$ ) for  $s$ - and  $p$ - state and radii for considered core nuclei and corresponding hypernuclei are tabulated in Table I. The calculated  $B_\Lambda$  is compared with available experimental data and we found a close agreement between them. This means the used parameter set is quite efficient to reproduce the experimental binding energy and ofcourse we can use it to make more calculations related to magicity in hypernuclei. Since, we are dealing with closed shell hypernuclei and hence our RMF calculations is restricted to spherical symmetric.

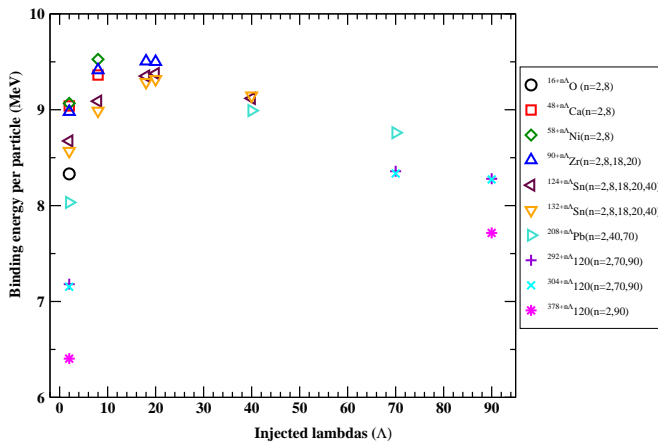


FIG. 1: (color online) Binding energy per particle for triply magic multi- $\Lambda$  hypernuclei.

The addition of  $\Lambda$  hyperon to normal nuclei enhances the binding and shrinks the core of the system. This is because of glue like role of  $\Lambda$  hyperon that residing on the  $s$ -state for most of the time. These observations are shown in Table I. Binding energy of hypernuclei are larger than their normal counterparts and a reduction in total radius ( $r_{total}$ ) of hypernuclei is observed, that means the  $\Lambda$  particle makes the core compact with increasing binding. For example, the total radius of  $^{16}O$  and  $^{209}Pb$  is 2.541 and 5.624 fm, which reduce to 2.536 and 5.616 fm by addition of single  $\Lambda$  into the core of  $O$  and  $Pb$ , respectively. Moreover, for the sake of comparison with experimental data, binding energy and radii of the hypernuclei produced by replacing the neutrons means having a constant baryon number are also framed in Table I and the shrinkage effect is also noticed. This results show that an important impact of  $\Lambda$  hyperon on binding as well as size of the system. The increasing value of  $B_{\Lambda}$  for  $s$ -state from light to superheavy hypernuclei confirming the potential depth of  $\Lambda$ -particle in nuclear matter which would be -28 MeV [61, 69].

### A. Stability of hypernuclei

Binding energy provides the detailed information of various elements corresponding to their stability. Binding energy per particle increases upto the element iron whose atomic number is 26 and mass number 57. The information provided by the binding energy per particle curve is that iron and its neighbouring elements (Ni) are most stable i.e. they neither undergo fission or fusion. Thus the significance of the binding energy per particle curve lies in the fact that it is an indicator of nuclear stability and thus helps in classifying the elements which undergo fission, fusion and radioactive disintegration. We noticed a similar pattern of binding energy per particle in hypernuclear regime also. The triply magic system is produced by addition of  $\Lambda$  magic number into the core of doubly shell closure such as  $^{16}O$ ,  $^{48}Ca$ ,  $^{58}Ni$ ,  $^{90}Zr$ ,  $^{124}Sn$ ,  $^{132}Sn$ ,  $^{208}Pb$ ,  $^{292}120$ ,  $^{304}120$ ,  $^{378}120$ . Binding energy per particle of considered systems confirming that nickel with 8  $\Lambda$ 's ( $^{56+8\Lambda}Ni$ )

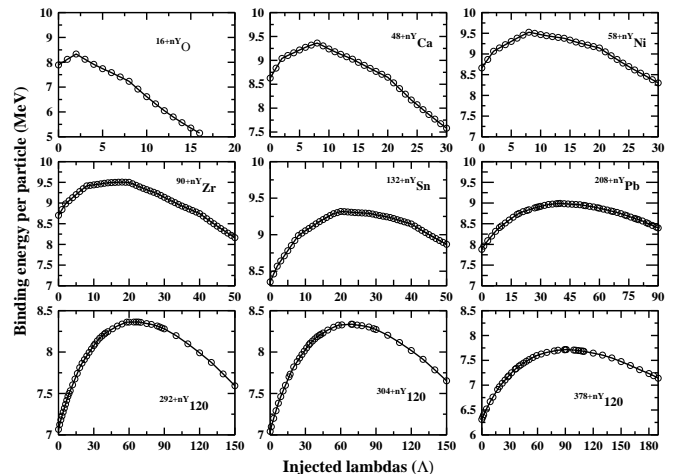


FIG. 2: Binding energy per particle for light to superheavy mass multi- $\Lambda$  hypernuclei.

being the most tightly bound hypernucleus ( $BE/A = 9.5$  MeV) as shown in Fig. 1. This results are in remarkable agreement with earlier predictions [61, 62].

### B. Binding energy and separation energy

To analyze the magic behaviour of lambda in multi- $\Lambda$  hypernuclei, we choose the nuclear core of doubly shell closure including predicted shell closure nuclei of superheavy mass region and then added the  $\Lambda$  hyperons. Initially, we look for the binding energy per particle with respect to added hyperons for considered hypernuclei and plotted in Fig. 2. The peak value of the graph corresponds to maximum stability for a particular hypernuclear system. It also explains that the injection of few  $\Lambda$  hyperons enhance the binding of the light mass hypernuclei, conversely further addition reduces the binding. However for heavy mass region, the  $BE/A$  increases with addition of large number of hyperons and form a most bound system but further addition decreases the binding energy gradually. This means certain number of added  $\Lambda$ 's to a particular nuclear core form a most stable system. For example, the injection of 2  $\Lambda$ 's provide a maximum stability to  $^{16}O$ . Along the similar line a maximum binding is observed for  $^{48}Ca$  with  $\Lambda = 8$  and this number goes to 90 for superheavy core. In this way, we extract certain numbers of added  $\Lambda$ 's that is 2, 8, 18, 20, 40, 70, 90 which provide maximum stability for the considered systems (i.e.  $^{16+2\Lambda}O$ ,  $^{48+8\Lambda}Ca$ ,  $^{58+8\Lambda}Ni$ ,  $^{90+18\Lambda}Zr$ ,  $^{124+20\Lambda}Sn$ ,  $^{132+20\Lambda}Sn$ ,  $^{208+40\Lambda}Pb$ ,  $^{292+68\Lambda}120$ ,  $^{304+70\Lambda}120$ ,  $^{378+90\Lambda}120$ ) and these numbers may correspond to  $\Lambda$  magic number in multi- $\Lambda$  hypernuclei. But, there exist several other strong signatures of marking the magic number such as; separation energy, shell gaps, pairing energy etc. Therefore, to analyze the actual behaviour of magicity, we make the analysis of such relevant parameters. In this regard, we estimate one- and two-lambda separation energy  $S_{\Lambda}$ ,  $S_{2\Lambda}$ , which are known to be first insight of shell closure. In analogy of nucleonic sector, the magic

TABLE I: The calculated total binding energy and binding energy per particle for single- $\Lambda$  hypernuclei and their normal counter parts are listed here. The  $\Lambda$  binding energy for  $s$ - and  $p$ -state of considered hypernuclei are also mentioned and compared with available experimental values [70], are given in parentheses. The radii are also displayed. Energies are given in unit of MeV and radii are in fm.

Nuclei / Hypernuclei	BE	BE/A	$B_{\Lambda}^s$	$B_{\Lambda}^p$	$r_{ch}$	$r_{total}$	$r_p$	$r_n$	$r_{\Lambda}$
$^{16}\text{O}$	126.27	7.89			2.674	2.541	2.555	2.527	
$^{16}_{\Lambda}\text{O}$	124.36	7.77	-12.09 (12.5 $\pm$ 0.35)	-2.66 (2.5 $\pm$ 0.5)	2.673	2.487	2.550	2.428	2.388
$^{17}_{\Lambda}\text{O}$	137.99	8.12	-11.98	-3.07	2.673	2.536	2.554	2.526	2.468
$^{40}\text{Ca}$	341.43	8.54			3.446	3.331	3.355	3.307	
$^{40}_{\Lambda}\text{Ca}$	344.16	8.60	-17.51 (18.7 $\pm$ 1.1)	-9.32 (11.0 $\pm$ 0.6)	3.439	3.292	3.346	3.262	2.693
$^{41}_{\Lambda}\text{Ca}$	358.65	8.75	-17.39	-9.46	3.444	3.315	3.352	3.304	2.737
$^{48}\text{Ca}$	414.17	8.63			3.444	3.496	3.359	3.591	
$^{48}_{\Lambda}\text{Ca}$	425.04	8.86	-18.75	-10.95	3.439	3.459	3.353	3.558	2.785
$^{49}_{\Lambda}\text{Ca}$	433.01	8.84	-18.94	-11.16	3.440	3.479	3.355	3.586	2.791
$^{56}\text{Ni}$	482.30	8.61			3.696	3.586	3.610	3.561	
$^{56}_{\Lambda}\text{Ni}$	487.47	8.71	-20.48	-12.67	3.695	3.560	3.609	3.533	2.816
$^{57}_{\Lambda}\text{Ni}$	502.96	8.82	-20.72	-12.89	3.689	3.567	3.603	3.555	2.817
$^{90}\text{Zr}$	783.17	8.70			4.249	4.245	4.179	4.297	
$^{90}_{\Lambda}\text{Zr}$	792.04	8.80	-21.28	-15.25	4.246	4.221	4.175	4.277	3.215
$^{91}_{\Lambda}\text{Zr}$	804.69	8.84	-21.37	-15.36	4.247	4.233	4.177	4.295	3.222
$^{124}\text{Sn}$	1048.19	8.45			4.642	4.753	4.580	4.866	
$^{124}_{\Lambda}\text{Sn}$	1060.81	8.55	-22.24	-17.10	4.633	4.729	4.571	4.849	3.493
$^{125}_{\Lambda}\text{Sn}$	1070.73	8.57	-22.28	-17.17	4.638	4.742	4.577	4.864	3.503
$^{132}\text{Sn}$	1102.69	8.35			4.689	4.854	4.631	4.985	
$^{132}_{\Lambda}\text{Sn}$	1118.13	8.47	-22.56	-17.65	4.680	4.830	4.620	4.969	3.570
$^{133}_{\Lambda}\text{Sn}$	1125.49	8.46	-22.60	-17.71	4.686	4.843	4.627	4.983	3.579
$^{208}\text{Pb}$	1639.32	7.88			5.499	5.624	5.448	5.736	
$^{208}_{\Lambda}\text{Pb}$	1655.85	7.78	-23.56 (26.3 $\pm$ 08)	-19.74 (21.3 $\pm$ 0.7)	5.492	5.604	5.441	5.719	4.067
$^{209}_{\Lambda}\text{Pb}$	1663.47	7.96	-23.54	-19.76	5.496	5.616	5.445	5.734	4.076
$^{292}\text{120}$	2063.09	7.06			6.271	6.322	6.225	6.389	
$^{292}_{\Lambda}\text{120}$	2103.33	7.12	-23.73	-20.94	6.262	6.306	6.216	6.376	3.316
$^{293}_{\Lambda}\text{120}$	2111.67	7.21	-23.59	-20.86	6.268	6.316	6.223	6.387	3.320
$^{304}\text{120}$	2140.81	7.04			6.302	6.417	6.258	6.519	
$^{304}_{\Lambda}\text{120}$	2184.09	7.19	-23.89	-21.03	6.298	6.403	6.253	6.507	3.272
$^{305}_{\Lambda}\text{120}$	2189.18	7.18	-23.79	-20.96	6.300	6.411	6.255	6.518	3.301
$^{378}\text{120}$	2385.44	6.31			6.714	7.144	6.678	7.350	
$^{378}_{\Lambda}\text{120}$	2432.02	6.11	-23.09	-20.81	6.896	7.344	6.863	7.543	3.642
$^{379}_{\Lambda}\text{120}$	2433.89	6.09	-23.43	-21.04	6.712	7.138	6.676	7.350	3.549

number in multi-hypernuclei may characterized by the large lambda shell gaps in single-particle energy levels. The extra stability given by certain number of introduced  $\Lambda$ 's can also be detect from sudden fall in  $\Lambda$  separation energy. Therefore, on quest of magicity in multi- $\Lambda$  hypernuclei, one- and two-lambda separation energy is estimated using the following expressions;

$$S_{\Lambda}(N, Z, \Lambda) = BE(N, Z, \Lambda) - BE(N, Z, \Lambda - 1)$$

and

$$S_{2\Lambda}(N, Z, \Lambda) = BE(N, Z, \Lambda) - BE(N, Z, \Lambda - 2).$$

These quantities are plotted in Fig. 3, 4, 5 and 6. For a lambda chain, the  $S_{\Lambda}$  and  $S_{2\Lambda}$  becomes larger with increasing number of lambda  $\Lambda$ . For a fixed  $Z, N$ ;  $S_{\Lambda}$  and  $S_{2\Lambda}$  decrease gradually with lambda number. A sudden decrease of  $S_{\Lambda}$  and  $S_{2\Lambda}$  just after the magic number in lambda chain like as neutron chain indicates the occurrence of  $\Lambda$  shell closure. The sudden fall of  $S_{\Lambda}$  at  $\Lambda = 2, 8, 14, 18, 20, 28, 34, 40, 50, 58, 68, 70$  and  $82$  can clearly be seen in considered hypernuclear candidates revealing a signature of magic character. Moreover,  $\Lambda = 14$  and  $28$  are observed only in light mass mulit- $\Lambda$  hypernuclei, even  $\Lambda = 28$  does not show pronounced energy separation.

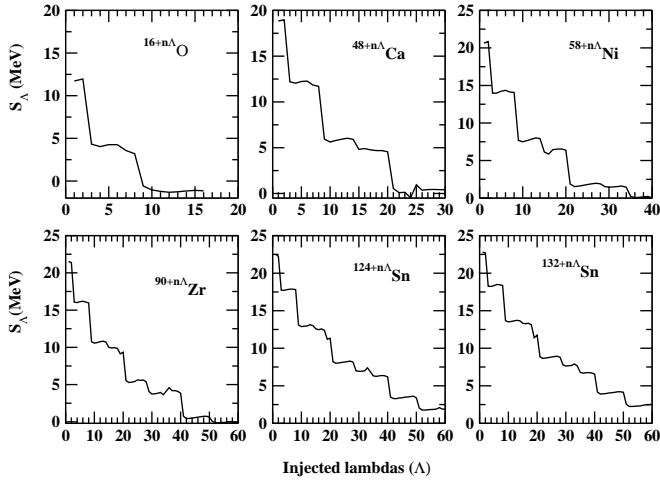


FIG. 3: One lambda separation energy for medium mass multi- $\Lambda$  hypernuclei.

However, a good strength of sudden fall of  $S_\Lambda$  at  $\Lambda = 34$  and  $58$  is clearly observed in heavy and superheavy mass region.

Two-lambda separation energy provides more strong signature to quantify shell closure due to absence of odd-even effects. Figures 5 and 6 reveal that sudden fall of  $S_{2\Lambda}$  at  $\Lambda = 2, 8, 14, 18, 20, 28, 34, 40, 50, 58, 68, 70$  and  $82$  as observed in considered multi- $\Lambda$  hypernuclear candidates. These certain numbers corresponds to  $\Lambda$  magic number in multi- $\Lambda$  hypernuclei and form a triply magic system with doubly magic core. This is the central theme of the paper. The significant falls of  $S_\Lambda$  and  $S_{2\Lambda}$  at  $\Lambda = 14$  is appeared in Ca and Ni hypernuclei. The lambda number 28 seems to be very much feeble magic number, contrary to nucleonic sector. The another new lambda number 68 suppose to be semi-magic arises due to subshells closure. For the sake of clear presentation of the results, we also make the analysis for two-lambda shell gaps ( $\delta_{2\Lambda}$ ) and plotted as a function of added  $\Lambda$ 's.

Summarizing the above results, we may say that based on one- and two-lambda separation energies  $S_\Lambda$  and  $S_{2\Lambda}$ , the signatures of the magicity in RMF appears at  $2, 8, 14, 18, 20, 28, 34, 40, 50, 58, 68, 70$  and  $82$ . The lambda number 28 and 68 are appeared in light and heavy hypernuclei, respectively and suppose to be feeble magic number.

### C. Two-lambda shell gap

The change of the two-lambda separation energies can also be quantified by the second difference of the binding energies, i.e., two-lambda shall gap which is expressed by:

$$\begin{aligned}\delta_{2\Lambda}(N, Z, \Lambda) &= 2BE(N, Z, \Lambda) - BE(N, Z, \Lambda + 2) - BE(N, Z, \Lambda - 2) \\ &= S_{2\Lambda}(N, Z, \Lambda) - S_{2\Lambda}(N, Z, \Lambda + 2).\end{aligned}$$

A peak of two-lambda shell gaps indicates the drastic change of the two-lambda separation energies; which is used as one of the significant signature of magic number. The two-lambda shell gaps  $\delta_{2\Lambda}$ , for all considered hypernuclei as a function of added  $\Lambda$  hyperons are shown in Fig 7. A peak at certain  $\Lambda$

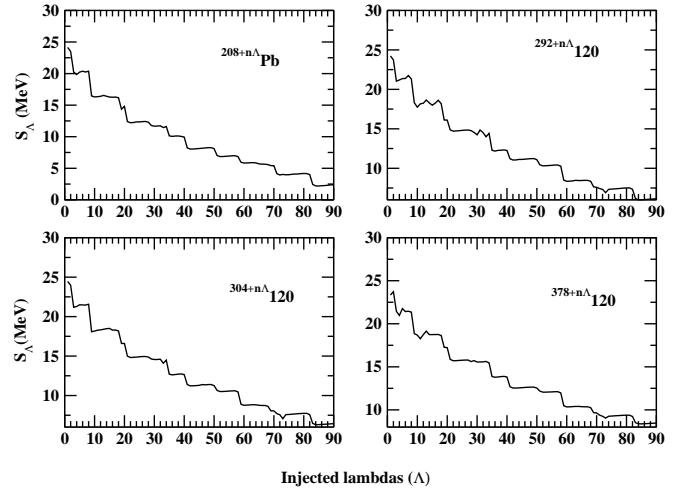


FIG. 4: Same as Fig. 3 but for heavy to superheavy mass multi- $\Lambda$  hypernuclei.

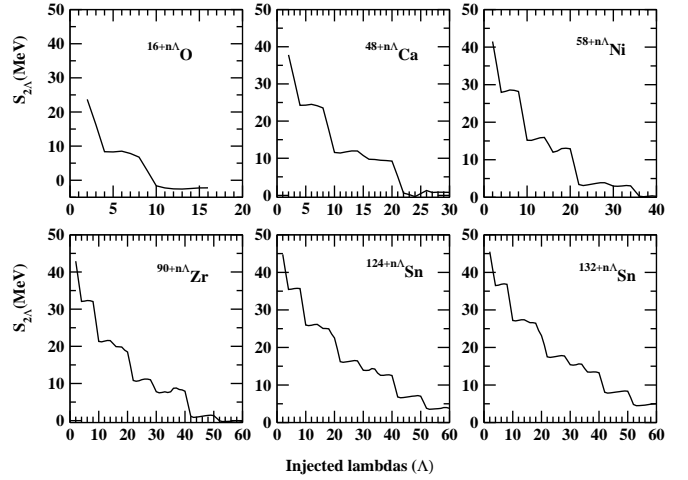


FIG. 5: Two lambda separation energy for medium mass multi- $\Lambda$  hypernuclei.

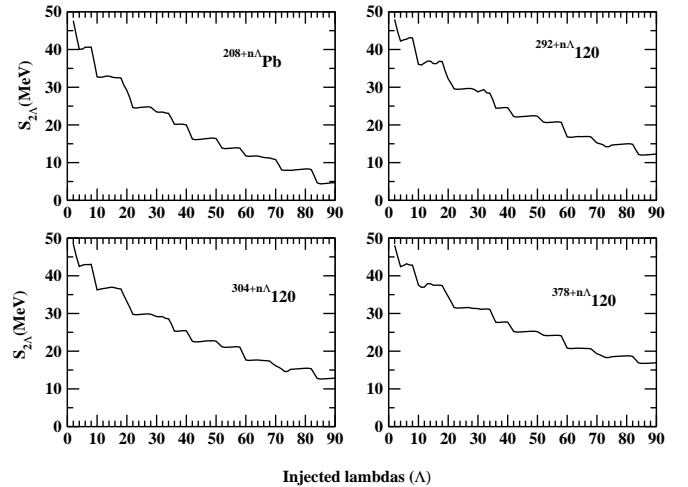


FIG. 6: Same as Fig. 5 but for heavy to superheavy mass multi- $\Lambda$  hypernuclei.

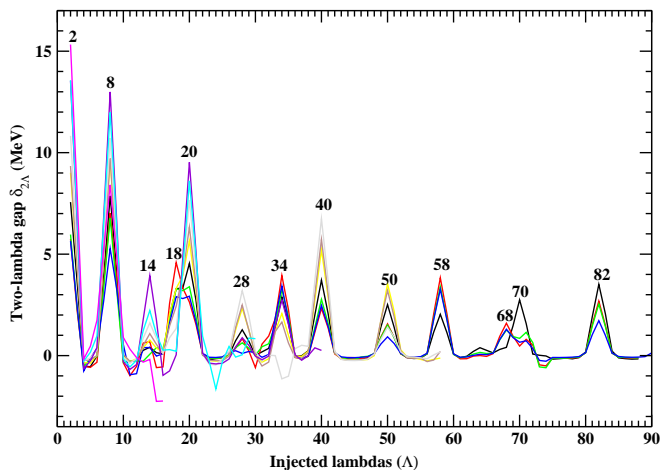


FIG. 7: (color online) Two lambda shell gap is shown for considered multi- $\Lambda$  hypernuclei.

number suggests the existence of lambda shell closure. However, the quality of magic number is represented by sharpness as well as magnitude of the peak. Figure. 7 reveals that the magnitude of the peak is found to be largest at  $\Lambda = 2, 8, 20, 40$  indicating the strong shell closures. Further, the peaks appeared at  $\Lambda = 14, 18, 28, 34, 50, 58, 70$  and  $82$  indicate the respective lambda magic number. Moreover, a peak with a very small magnitude is also appeared at  $\Lambda = 68$  due to closure of subshell ( $2d_{3/2}$ ) revealing  $\Lambda$  semi-magic number. A peak with small magnitude is seen at  $\Lambda = 28$  representing a feeble lambda magic number, contrary to nucleonic magic number. Pronounced peak is appeared at  $\Lambda = 34$  and  $58$  indicating a strong  $\Lambda$  closed shells.

#### D. Density profile and bubble structure

A hypernucleus is a composed system of nucleons and hyperons and hence the gross structure of hypernucleus can be described by density distribution of nucleons as well as hyperons. It is well known and has mentioned earlier that the addition of a  $\Lambda$  hyperon makes the nuclear core compact with increasing binding as well as density. Therefore, it is important to study the effects of large number of added  $\Lambda$  hyperons on the nuclear density. Due to addition of hyperons, the magnitude of total density increases with increasing number of  $\Lambda$ 's as shown in Fig. 8. On view the density profile, one can examine the most interesting feature of nuclei i.e. bubble structure, which measure the depression of central density and has already been observed in light to superheavy mass region [60, 71–73]. It is to be noticed that several factors, including pairing correlations [73], tensor force [74, 75] and dynamic shape fluctuations [76–78] turn out to have influence on depression of central density. The exotic structures like bubble and halo have been recently studied in  $\Lambda$ -hypernuclei [60, 79].

Owing to weaker  $\Lambda\Lambda$  attraction compared to the nucleon-nucleon one the lambda hyperons are more diffuse in a nu-

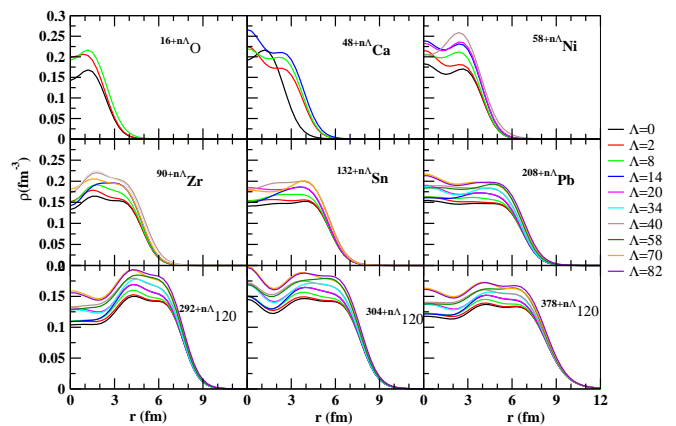


FIG. 8: (color online) Total (Nucleon plus lambda) density for considered triply magic hypernuclei with  $\Lambda=0, 2, 8, 14, 20, 34, 40, 58, 70$  and  $82$ .

cleus than nucleons and thus generating a hyperon density about  $1/3$  smaller than the nucleonic density. Thus, it becomes quite important to look for the effect of large number of hyperons on neutron and proton density distributions. Since, there is no change of nucleon number and hence no anomalous effect of introduced  $\Lambda$ 's on neutron, proton densities is observed, individually. But the total density of the system is largely affected due to increasing number of  $\Lambda$ 's into the core. In considered multi-hypernuclei, the nucleonic core of some of them shows the depression of central density for example  $^{16}O$ ,  $^{90}Zr$ ,  $^{292}120$ ,  $^{304}120$  and  $^{378}120$  as predicted earlier also [60, 72]. It is found that the injected  $\Lambda$ 's reduce the depression of central density. For example, the depression of central part in  $^{16}O$  is reduced by injection of 2  $\Lambda$ 's and further more by 8  $\Lambda$ 's. The  $\Lambda$  particle attracts the nucleons towards the centre enhancing the central density and as a result remove the bubble structure partially or fully as reflected in Fig. 8. Therefore, it is one of the important implication of  $\Lambda$  particle to the nuclear system. Beyond the bubble structure, no anomalous behaviour of total density (core +  $\Lambda$ ) in triply magic system is reported.

#### E. Spin-orbit interaction and mean field potentials

The spin-orbit interaction plays a significant role in reproducing the results quantitatively. It is the beauty of RMF in which the spin-orbit splitting is built-in naturally with exchange of scalar and vector mesons and thus describe a nuclear fine structure. It is not limited only to nuclei or superheavy nuclei but appears in hypernuclei also, however the strength of interaction is weaker than normal nuclei [56, 80, 81]. It is clearly seen from Figs. 9 that the spin-orbit potential for lambda hyperon is weaker than their normal counterparts and our results are consistent with theoretical predictions and experimental measurements [82–84]. Here, nucleon ( $V_{so}^N$ ) and lambda ( $V_{so}^\Lambda$ ) spin-orbit interaction potentials are calculated for considered triply magic multi-hypernuclei. It is also conclude that the addition of  $\Lambda$ 's affects the nucleon as well

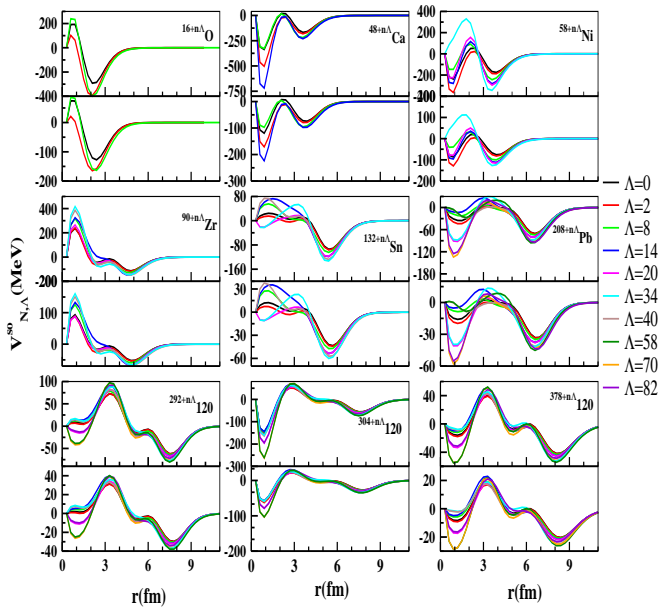


FIG. 9: (color online) Spin-orbit interaction potentials of nucleon and lambda for considered triply magic hypernuclei with  $\Lambda=0, 2, 8, 14, 20, 34, 40, 58, 70$  and  $82$ . The upper part in each panel represents the nucleonic spin-orbit and the lower one representing the lambda spin-orbit interaction.

as  $\Lambda$  spin-orbit potential to a great extent.

The nucleon ( $V_N$ ) and lambda ( $V_\Lambda$ ) mean field potentials are also investigated and plotted as a function of radial parameter shown in Fig. 10. The total depth of  $\Lambda$  mean field potential is found to be around  $-30$  MeV, which is in agreement with existing experimental data [84]. It is to mention that the additions of  $\Lambda$ 's affects the depth of both nucleon as well as lambda mean potentials. The nucleonic potential depth in multi-lambda hypernuclei is approx to  $-80$  MeV to  $-90$  MeV. The shape of lambda potential looks like to be same as nucleonic potential and only the amount of depth is different. It is also to be noticed that the nucleonic potential looks like as V-shape type and shows the maximum depth around  $-90$  MeV at  $r = 4$  fm, while this amount of depth reaches to  $-70$  MeV at  $r = 0$  fm for  $^{292}120$ . It indicates a relatively low concentration of the particles at central region ( $r = 0$ ) which is a direct consequence of depression of central density so-called bubble structure.

### F. Single-particle energies

Any kinds of change in a system can be observed from their single-particle energy levels. To analyze the impact of  $\Lambda$  hyperon on nucleon single-particle energy levels, the filled neutron and proton levels for Ca hypernuclei are plotted as a function of added hyperons as shown in Fig. 11. Figure 11 reveals that the neutron and proton energy levels goes dipper with addition of  $\Lambda$ 's as a result increase the stability of the system. The added hyperons increase the nucleon separation energy and as a result form a more bound system with increas-

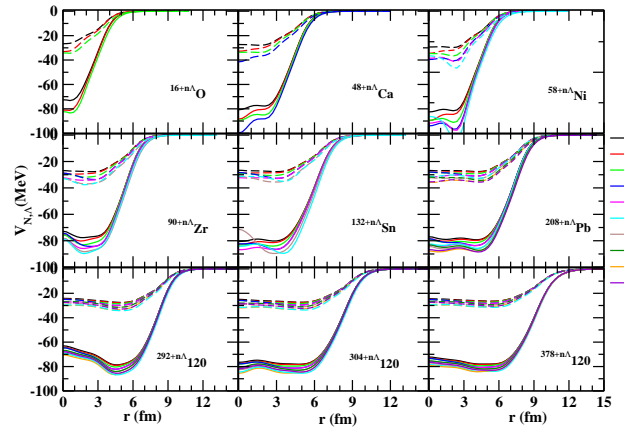


FIG. 10: (color online) Total mean field potentials for considered triply magic hypernuclei with  $\Lambda=0, 2, 8, 14, 20, 34, 40, 58, 70$  and  $82$ . Dashed lines represents the lambda mean potential and the nucleon potential is shown by solid line.

ing binding then their normal counter parts, which also leads to an extension of drip-line [29]. For example, neutron  $s_{1/2}(n)$  level has an energy of about  $-54.037$  MeV for the core of Ca hypernucleus, while this amount reaches to  $-62.499$  MeV for  $^{48+18\Lambda}Ca$  system with  $18 \Lambda$ 's. Also, a same trend is observed for proton levels where,  $s_{1/2}(p)$  has an energy  $51.787$  MeV for the core of Ca hypernuclei and this value reaches to  $-60.0477$  MeV with addition of  $18 \Lambda$ 's. This results show that the  $\Lambda$  hyperons draw the nuclear system towards more stability with increasing strangeness. Moreover, the same trend of neutron and proton energy levels is observed for other multi hypernuclei where both the levels would go dipper with increasing number of  $\Lambda$  hyperon to nucleonic core but we do not make a plot for the same. A inversion of proton levels is seen, where  $d_{3/2}$  fill faster than  $s_{1/2}$  and this type of filling is also observed in lambda levels.

Further, we analyze the lambda single-particle energy levels for  $^{48+n\Lambda}Ca$ ,  $^{208+n\Lambda}Pb$  and  $^{304+n\Lambda}120$  hypernuclei to extract the lambda shell gaps for confirming the  $\Lambda$  magic number. The lambda energy levels as function of added  $\Lambda$ 's are given in Fig. 11, 12, 13. The filling of  $\Lambda$ 's is same as the nucleons following the shell model scheme with lambda spin-orbit interaction. It is observed that the single-particle gap of spin-orbit splitting in lambda levels is smaller than the nucleons due to weakening strength of lambda spin-orbit interaction. By analyzing the lambda single-particle energy levels of Ca hypernuclei it is found that large energy gap exist in  $1d_{5/2}$  to  $1d_{3/2}$  or  $2s_{1/2}$  and that's why lambda magic number 14 is emerged. Further,  $2s_{1/2}$  and  $1d_{3/2}$  are very much close to each other due to weaker strength of  $\Lambda$  spin-orbit interaction. However,  $\Lambda = 20$  is clearly seen due to large energy gap by  $f_{7/2}$  to lower orbital. In case of Pb, the large shell gaps for  $\Lambda = 2, 8, 18, 20, 28, 34, 40, 50, 58, 70$  and  $82$  is appeared. However, the single-particle gap for lambda number 28 is not so strong as compared to others suggesting the feeble magic number. The inversion of normal level scheme is noticed and the higher levels fill faster than lower one and hence this types of filling is responsible to emerge the new more magic number. For exam-

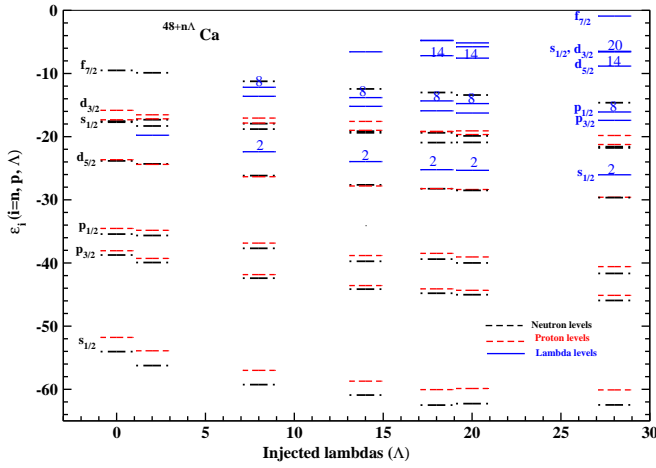


FIG. 11: (color online) Single-particle energy levels for triply magic Ca multi-hypernuclei for  $\Lambda = 2, 8, 14, 18, 20$  and  $28$ .

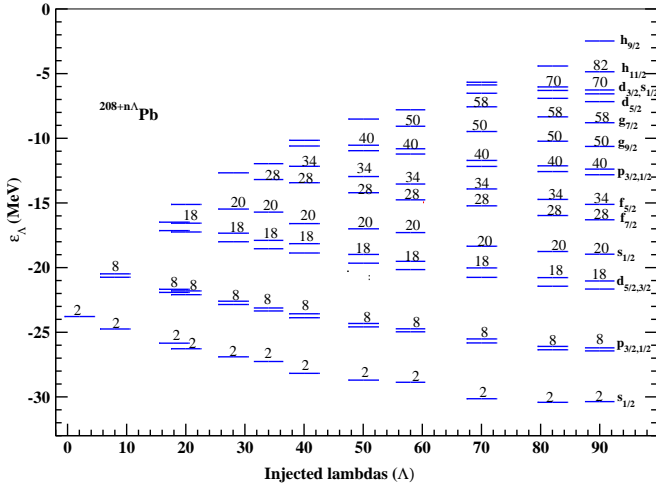


FIG. 12: (color online) Single-particle energy levels for triply magic Pb multi-hypernuclei for  $\Lambda = 2, 8, 18, 20, 28, 34, 40, 50, 58, 70, 82$  and  $90$ .

ple, the filling of  $1d_{3/2}$  before  $2s_{1/2}$  shows a shell gap at  $\Lambda = 18$ . Along the similar line, due to inversion between  $\{1f_{5/2}, 2p_{3/2}\}$  and  $\{1g_{7/2}, 2d_{5/2}\}$  the  $\Lambda$  closed shells  $34$  and  $58$  is observed, respectively. In case of superheavy multihypernuclei, large single-particle shell gaps are appeared for lambda number  $2, 8, 18, 20, 34, 40, 50, 58, 70$  and  $82$ . It is quite worth to notice that pronounced energy gaps is noticed in  $^{208}\text{Pb}$  and  $^{304}120$  at  $\Lambda = 34, 58$  are being suggested to be strong  $\Lambda$  shell closure. The sharp peaks observed in  $\delta_{2\Lambda}$  at  $\Lambda = 2, 8, 20, 34, 40$  and  $58$  is clearly reflected from lambda single-particle energies, where a large energy gap is exist for the filling of these number of lambda hyperons.

### G. Magicity

Various signatures of the evolution of magic shell gaps have been discovered across the nuclear landscape during the past

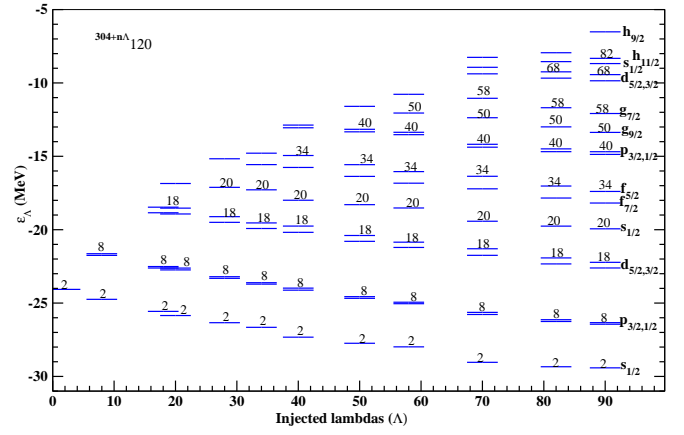


FIG. 13: (color online) Single-particle energy levels for triply magic  $^{304}120$  multi-hypernuclei for  $\Lambda = 2, 8, 18, 20, 28, 34, 40, 50, 58, 70, 82$  and  $90$ .

TABLE II: Lambda magic number produced in various considered multi-hypernuclei are tabulated here.

Hypernuclei	Lambda magic number									
$^{16+n\Lambda}\text{O}$	2	8	-	-	-	-	-	-	-	-
$^{48+n\Lambda}\text{Ca}$	2	8	14	-	20	-	-	-	-	-
$^{58+n\Lambda}\text{Ni}$	2	8	14	-	20	28	34	-	-	-
$^{90+n\Lambda}\text{Zr}$	2	8	14	-	20	28	-	40	50	-
$^{124+n\Lambda}\text{Sn}$	2	8	14	-	20	28	34	40	50	-
$^{132+n\Lambda}\text{Sn}$	2	8	14	-	20	28	34	40	50	-
$^{208+n\Lambda}\text{Pb}$	2	8	-	18	20	28	34	40	50	58
$^{292+n\Lambda}120$	2	8	-	18	-	28	34	40	50	58
$^{304+n\Lambda}120$	2	8	-	18	20	28	34	40	50	58
$^{378+n\Lambda}120$	2	8	14	18	20	-	34	40	50	58

few decades [37, 38] such as (i) A large binding energy then neighbouring nuclides, (ii) Sudden fall at separation energy, (iii) A large shell gap, etc. It becomes therefore quite relevant to extend the prediction of magic numbers to the hypernuclear chart. Looking for the magic behaviour firstly, we emphasize on binding of some selected nuclei whose nucleonic core is doubly magic such as  $O, Ca, Ni, Zr, Sn, Pb$  and  $120$ . Some certain number of  $\Lambda$  hyperon binds the nuclear core with maximum stability that may correspond to  $\Lambda$  magic number in hypernuclei and might form a triple magic system with doubly magic nuclear core as initially discussed in Ref. [85] and recently in Ref. [79]. For example,  $\Lambda = 2$ , produce a maximum binding for  $^{16}\text{O}$  and  $^{48}\text{Ca}$  reveal the maximum binding with  $\Lambda = 8$ . Also,  $^{378}120$  shows a peak binding on addition of  $90 \Lambda$ 's. In this way, we extract some lambda number which are  $2, 8, 18, 20, 40, 70, 90$  produce a maximum stability for their particular system and suppose to be  $\Lambda$  magic number as much as close to harmonic oscillator number. But several other strong signatures are exist to identify the magicity and we make the analysis in this direction to look out the correct  $\Lambda$  magic number. After analyzing the  $S_{\Lambda}$  and  $S_{2\Lambda}$ , for considered light to superheavy mass multi-hypernuclei it is noticed that a sudden fall is observed at  $\Lambda = 2, 8, 14, 20, 28, 34, 40,$



50, 58, 68, 70 and 82. And hence, the analysis suggest that these numbers are supposed to be  $\Lambda$  magic number in multi-lambda hypernuclei and form a triply magic system having doubly magic nucleonic core.

In order to identify the  $\Lambda$  magic number strongly, two-lambda shell gaps is examined which provide more strong signature of magicity and favoured  $S_{2\Lambda}$ . Pronounced peak in two-lambda shell gap is observed at  $\Lambda = 2, 8, 20$  and  $40$  indicating a strong shell closure. The peaks observed with a significant magnitude at  $\Lambda = 14, 18, 34, 50, 58, 70$  and  $82$  indicating a shell closure also. Further to testify, we look for the lambda shell gaps by examining the single-particle energy levels. We noticed that a large single-particle gap is appeared in  $^{208}\text{Pb}$  hypernucleus at  $\Lambda = 2, 8, 18, 20, 28, 34, 40, 50, 58$  and  $70$  confirming the lambda magic number. The analysis of single-particle energy levels for  $^{378}120$  multi hypernuclei clear the results by showing a large energy gap in  $2, 8, 18, 20, 34, 40, 50, 58, 70$  and  $82$ . It is to mention that a significant shell gap is observed for  $34$  and  $58$  suggesting a strong  $\Lambda$  shell closure. The inversion of normal level scheme is responsible to emerge the  $\Lambda$  magic number  $34$  and  $58$ . The experimentally confirmation of nucleonic shell closure of  $34$  supports our predictions [86, 87]. The nucleonic number  $14, 16, 18$  and  $32$  have also been in discussion and expected to be shell closure [88–91]. In addition, nucleon number  $16$  and  $32$  have also been experimentally confirmed in exotic nuclei as a new neutron magic number [92, 93]. Therefore, it is concluded that the  $\Lambda$  magicity quite resembles with the nuclear magicity and it is expected that our predictions might be used as significant input to make the things clear regarding new sub shell closure. The predicted  $\Lambda$  magic number in multi-hypernuclei are framed in Table II. The present lambda magic numbers are quite agreeable with the prediction of Ref. [85] and Ref. [79] where Bruckner-Hartee Fock calculations using the lambda density functional have been made. It is clear from the plot of  $\delta_{2\Lambda}$ , that  $34, 58$  and  $70$  have peaks of great magnitude, while  $68$  in a feeble magnitude and suppose to be subshell closure. Moreover, strong nucleonic magic number  $28$  is observed very feeble in lambda magicity. It is to mention that the lambda number  $14$  is appeared in medium mass hypernuclei, on contrary to this  $18$  is observed in superheavy mass multi hypernuclei.

#### IV. SUMMARY AND CONCLUSION

In summary, we have suggested the possible  $\Lambda$  magic number i.e.  $2, 8, 14, 18, 20, 28, 34, 40, 50, 58, 68, 70, 82$  in

multi- $\Lambda$  hypernuclei within the relativistic mean field theory with effective  $\Lambda N$  as well as  $\Lambda\Lambda$  interactions. The survey of  $\Lambda$  magic number is made on the basis of binding energy, one- and two-lambda separation energies  $S_\Lambda, S_{2\Lambda}$ , and two-lambda shell gaps  $\delta_{2\Lambda}$ . It is noticed that pronounced single particle energy gap is observed for lambda number  $34$  and  $58$  in  $\text{Pb}$  and superheavy multi hypernuclei representing the strong  $\Lambda$  magic number. Our predictions are strongly supported by nuclear magicity, where nucleon number  $34$  is experimentally confirmed as a neutron shell closure [86, 87]. It is expected that the weakening strength of lambda spin-orbit interaction potential is responsible for emerging the new lambda magic number. The predicted  $\Lambda$  magic numbers are in remarkable agreement with earlier predictions [79, 85] and hypernuclear magicity quite resembles with nuclear magicity. In the analogy of nuclear stability, we noticed a similar pattern of binding energy per particle in hypernuclear regime and  $\text{Ni}$  hypernucleus with  $8 \Lambda$ 's is found to be most tightly bound triply magic system in hypernuclear landscape. The addition of  $\Lambda$  hyperons have significant impact on nucleon distribution and remove the bubble structure partially or fully. The spin-orbit interaction potentials and mean field potentials is also studied for predicted triply magic hypernuclear systems and the added  $\Lambda$ 's affect both the potential to a large extent. The present results may be used as a significant input to produce the triply magic hypernuclei in laboratory in future. It is also concluded that the addition of  $\Lambda$  hyperons draw the nuclear system towards more stability with increasing strangeness. We noticed that the core of superheavy nuclei has more affinity to absorb large number of hyperons. This means such systems are able to simulate the strange hadronic matter containing large number of heavy hyperons such as  $\Sigma$ 's and  $\Xi$ 's including several  $\Lambda$ 's and the formation of such systems has large implication in nuclear-astrophysics.

#### V. ACKNOWLEDGMENTS

One of the authors (MI) acknowledge the hospitality provided by Institute of Physics, Bhubaneswar during the work.

- 
- [1] H. Bando, T. Motoba and J. Zofka, Int. J. Mod. Phys. A **5**, 4021 (1990).
  - [2] Y. Tan, X. Zhong, C. Cai, P. Ning, Phys. Rev. C **70**, 054306 (2004).
  - [3] B. Lu, E. Zhao and S. Zhou, Phys. Rev. C **84**, 014328 (2011).
  - [4] M. Rayet, Ann. Phys. **102**, 226 (1976).
  - [5] M. Rayet, Nucl. Phys. A **367**, 381 (1981).
  - [6] D. E. Lansky, Phys. Rev. C **58**, 3351(1998).
  - [7] J. Meng, H. Toki, S. G. Zhou et al., Prog. Part. Nucl. Phys. **57**, 470 (2006).
  - [8] X.-R. Zhou, H.-J. Schulze, H. Sagawa, C.-X. Wu and E.-G. Zhao, Phys. Rev. C **76**, 034312 (2007).
  - [9] H. F. Lü, Chin. Phys. Lett. **25**, 3613 (2008).
  - [10] N. Guleria, S. K. Dhiman and R. Shyam, Nucl. Phys. A **886**, 71

- (2012).
- [11] F. Minto and K. Hagino, *Phys. Rev. C* **85**, 024316 (2012).
- [12] A. Bouyssy, *Nucl. Phys. A* **381**, 445 (1982).
- [13] J. Mares and J. Zofka, *Z. Phys. A* **333**, 209 (1989).
- [14] M. Rufa, J. Schaffner, J. Maruhn H. Stöcker and W. Greiner and P.-G. Reinhard, *Phys. Rev. C* **42**, 2469(1990).
- [15] J. Schaffner, C. Greiner and H. Stöcker, *Phys. Rev. C* **46**, 322 (1992).
- [16] J. Mares and J. Zofka, *Z. Phys. A* **345**, 47 (1993).
- [17] J. Schaffner, et. al., *Ann. Phys.* **235**, 35 (1994).
- [18] E. N. E. Van Dalen, G. Colucci and A. D. Sedrakian, *Phys. Lett. B* **734**, 383 (2014).
- [19] E. Hiyama, M. Kamimura, Y. Yamamoto, T. Motoba and T. A. Rijken, *Prog. Theo. Phys. Suppl.* **185**, 106 (2010).
- [20] E. Hiyama, *Few. Body. Syst.* **53**, 189 (2012).
- [21] H. Nemura, S. Shinmura, Y. Akaishi, and Khin Swe Myint, *Phys. Rev. Lett.* **94**, 202502 (2005).
- [22] H. Nemura, S. Shinmura, Y. Akaishi, and Khin Swe Myint, *Nucl. Phys. A* **754**, 110c (2005).
- [23] A. Gal, *Few. Body. Syst.* **45**, 105 (2009).
- [24] A. Gal and D. J. Millener, *Phys. Lett. B* **701**, 342 (2011).
- [25] A. A. Usmani, *Phys. Rev. C* **73**, 011302(R) (2006).
- [26] A. A. Usmani and F. C. Khanna, *J. Phys. G: Nucl. Part. Phys.* **35**, 025105 (2008).
- [27] X.-R. Zhou, A. Polls, H. -J. Schulze, and I. Vidaña, *Phys. Rev. C* **78**, 054306 (2008).
- [28] I. Vidaña, A. Ramos and A. Polls, *Phys. Rev. C* **70**, 024306 (2004).
- [29] C. Samanta, P. Roy Chowdhury and D. N. Basu, *J. Phys. G: Nucl. and Part. Phys.* **35**, 065101 (2008).
- [30] D. E. Lenskoy and Y. Yamamoto, *Phys. Rev. C* **55**, 2330 (1997).
- [31] J. Cugnon, A. Lejeune and H.-J. Schulze, *Phys. Rev. C* **62**, 064308 (2000).
- [32] I. Vidana, A. Polls, A. Ramos and H.-J. Schulze, *Phys. Rev. C* **64**, 044301 (2001).
- [33] M. Goepfert-Mayer and J. Jensen, *Elementary Theory of Nuclear Shell Structure* (Wiley, New York, 1955; Inostrannaya Literatura, Moscow, 1958).
- [34] V. G. Solovov, *Theory of Atomic Nuclei* (Energoizdat, Moscow, 1981; Institute of Physics, Bristol, England, 1992).
- [35] S. G. Nilsson and I. Ragnarsson, *Shapes and Shells in Nuclear Structure* Cambridge University Press, Cambridge, England, (1995).
- [36] O. Sorlin, M.-G. Porquet, arXiv:0805.2561v1 (2008).
- [37] M. Bhuyan and S. K. Patra, *Mod. Phys. Lett. A* **27**, 1250173 (2012).
- [38] W. Zhang, J. Meng., S. Q. Zhang, L.S. Geng and H. Toki, *Nucl. Phys. A* **753**, 106 (2005).
- [39] V. M. Strutinsky, *Nucl. Phys. A* **95**, 420 (1967).
- [40] V. M. Strutinsky, *Nucl. Phys. A* **122**, 1 (1998).
- [41] S. K. Patra, R. K. Gupta and W. Greiner, *Mod. Phys. Lett. A* **12**, 1727 (1997).
- [42] T. Sil, S.K. Patra, B.K. Sharma, M. Centelles, and X. Vinas, *Phys. Rev. C* **69**, 044315 (2004).
- [43] K. Rutz, M. Bender, T. Bürvenich, T. Schilling, P.-G. Reinhardt, J. A. Maruhn, and W. Greiner, *Phys. Rev. C* **56**, 238 (1997).
- [44] S. K. Patra, C.-L. Wu, C. R. Prahara, and R. K. Gupta, *Nucl. Phys. A* **651**, 117 (1999).
- [45] J. Meng, H. Toki, S. Zhou, S. Zhang, W. Long, and L. Geng, *Prog. Part. Nucl. Phys.* **57**, 470 (2007).
- [46] S. K. Singh, M. Ikram and S. K. Patra, *Int. J. Mod. Phys. E* **22**, 1350001 (2013).
- [47] B. D. Serot, *Rep. Prog. Phys.* **55**, 1855 (1992).
- [48] Y. K. Gambhir, P. Ring and A. Thimet, *Ann. Phys. (NY)* **198**, 132 (1990).
- [49] P. Ring, *Prog. Part. Nucl. Phys.* **37**, 193 (1996).
- [50] B. D. Serot and J. D. Walecka, *Adv. Nucl. Phys.* **16**, 1 (1986).
- [51] J. Boguta and A. R. Bodmer, *Nucl. Phys. A* **292**, 413 (1977).
- [52] T. K. Jha, P. K. Raina, P. K. Panda and S. K. Patra, *Phys. Rev. C* **74**, 029903 (2007).
- [53] N. K. Glendenning, J. Schaffner, *Phys. Rev. Lett* **81**, 4564 (1998).
- [54] J. Schaffner, M. Hanauske, H. Stöcker and W. Greiner, *Phys. Rev. Lett.* **89**, 171101 (2002).
- [55] Y. Sugahara and H. Toki, *Prog. Theor. Phys.* **92**, 803 (1994).
- [56] D. Vretenar, W. Pošchl, G. A. Lalazissis and P. Ring, *Phys. Rev. C* **57**, R1060 (1998).
- [57] H. -F. Lü, J. Meng, S. Q. Zhang and S. G. Zhou, *Eur. Phys. J. A* **17**, 19 (2003).
- [58] H. Shen, F. Yang and H. Toki, *Prog. Theor. Phys.* **115**, 325 (2006).
- [59] M. T. Win and K. Hagino, *Phys. Rev. C* **78**, 054311 (2008).
- [60] M. Ikram, S. K. Singh, A. A. Usmani and S. K. Patra, *Int. J. Mod. Phys. E* **23**, 1450052 (2014).
- [61] J. Schaffner, C. B. Dover, A. Gal, C. Greiner, D. J. Millener and H. Stöcker, *Ann. Phys. (N.Y.)* **235**, 35 (1994).
- [62] J. Schaffner, C. B. Dover, A. Gal, C. Greiner and H. Stöcker, *Phys. Rev. Lett.* **71**, 1328 (1993).
- [63] N. K. Glendenning, D. Von-Eiff, M. Haft, H. Lenske and M. K. Weigel, *Phys. Rev. C* **48**, 889 (1993).
- [64] J. Mares and B. K. Jennings, *Phys. Rev. C* **49**, 2472 (1994).
- [65] M. Rufa, J. Schaffner, J. Maruhn, H. Stöcker and W. Greiner, *Phys. Rev. C* **42**, 2469 (1990).
- [66] G. A. Lalazissis, S. Karatzikos, R. Fossion, D. Pena Arteaga, A. V. Afanasjev and P. Ring, *Phys. Lett. B* **671**, 36 (2009).
- [67] M. Chiapparini, M. E. Bracco, A. Delfino, M. Malheiro, D. P. Menezes, C. Providencia, *Nucl. Phys. A* **826**, 178 (2009).
- [68] C. B. Dover and A. Gal, *Prog. Part. Nucl. Phys.* **12**, 171 (1984).
- [69] D. J. Millener, C. B. Dover and A. Gal, *Phys. Rev. C* **38**, 2700 (1988).
- [70] O. Hashimoto and H. Tamura, *Prog. Part. Nucl. Phys.* **57**, 564 (2006).
- [71] E. Khan et.al, *Nucl. Phys. A* **800**, 37 (2008).
- [72] J. Decharge, et., al. *Nucl. Phys. A* **716**, 55 (2003).
- [73] M. Grasso et. al., *Phys. Rev. C* **79**, 034318 (2009).
- [74] Y. Z. Wang, J. Z. Gu, Z. Y. Li, and Z. Y. Hou, *Eur. Phys. J. A* **15**, 49 (2013).
- [75] H. Nakada, K. Sugimura and J. Margueron, *Phys. Rev. C* **87**, 067305 (2013).
- [76] J. M. Yao, H. Mei and Z. P. Li, *Phys. Lett. B* **723**, 459 (2013).
- [77] J. M. Yao, S. Baroni, M. Bender and P.-H. Heenen, *Phys. Rev. C* **86**, 014310 (2012).
- [78] X. Y. Wu, T. M. Yao, and Z. P. Li, *Phys. Rev. C* **89**, 017304 (2014).
- [79] E. Khan, J. Margueron, F. Gulminelli and Ad. R. Raduta, *Phys. Rev. C* **92**, 044313 (2015).
- [80] J. Boguta and S. Bohrmann, *Phys. Lett. B* **102**, 93 (1981).
- [81] J. V. Noble, *Phys. Lett. B* **89**, 325 (1980).
- [82] R. Brockmann and W. Weise, *Phys. Lett. B* **69**, 167 (1977).
- [83] S. Ajimura et. al., *Phys. Rev. Lett.* **86**, 4255 (2001).
- [84] C. M. Keil, F. Hoffmann and H. Lenske, *Phys. Rev. C* **61**, 064309 (2000).
- [85] J. Mares and J. Zofka, *Z. Phys. A* **333**, 209 (1989).
- [86] D. Steppenbeck, S. Takeuchi, N. Aoi, P. Doornenbal, M. Matsushita et.al., *Nature* **502**, 207 (2013).
- [87] P. Maierbeck et. al., *Phys. Lett. B* **675**, 22 (2009).
- [88] T. R. Rodriguez, J. L. Egido, *Phys. Rev. Lett.* **99**, 062501 (2007).

[89] A. Ozawa et. al., Phys. Rev. Lett. **84**, 5493 (2000).

[90] R. Kanungo et.al., Phys. Lett. B **528**, 58 (2002).

[91] Jia. Jie Li, J. Margueron, W. H. Long, N. V. Giai, Phys. Lett. B **753**, 97 (2016).

[92] R. Kanungo et. al., Phys. Rev. Lett. **102**, 152501 (2009).

[93] F. Wienholtz et. al., Nature **498**, 346 (2013).